

# Radiation Load to the SNAP CCD

N.V. Mokhov, I.L. Rakhno, S.I. Striganov, T.J. Peterson

*Fermilab, P.O. Box 500, Batavia, IL 60510, USA*

August 6, 2003

## **Abstract**

Results of an express Monte Carlo analysis with the MARS14 code of radiation load to the CCD optical detectors in the Supernova Acceleration Project (SNAP) mission presented for realistic radiation environment over the satellite orbit.

# 1 Introduction

The purpose of the Supernova Acceleration Project (SNAP) is probing dark energy by observations of Type Ia supernovae in a 3-year space-based mission [1]. One of the crucial technical issues is radiation load to the critical devices, a charge-coupled device (CCD) photodetector first of all. It is calculated here with the MARS14 code [2] for a simple geometry model and radiation environment averaged over the SNAP orbit.

## 2 Radiation Environment at the SNAP Orbit

The orbit of the satellite (inclination 26.3 degrees, apogee 152830 km, perigee 10000 km) is taken into account by means of the codes CREME96 [3] and SPENVIS [4]. SPENVIS is used to represent electron component of Earth's radiation belts while CREME96 is used to represent galactic cosmic rays (GCR) and solar flares. The most significant limitation consists of the maximum apogee allowed in the code CREME96, namely 100000 km. Therefore the contribution from GCR is calculated here for a restricted orbit with apogee of 100000 km. All the spectra of incoming radiation are calculated taking into account geomagnetic shielding in the Earth's geomagnetic field.

The codes used allow us to divide the cosmic radiation into four categories:

1. Protons trapped in radiation belts.
2. Electrons trapped in radiation belts.
3. Primary (non-trapped) protons and heavy ions.
4. Primary (non-trapped) electrons.

Calculated orbit-averaged energy spectra for these components are shown in Fig. 1 at solar minimum and at the largest solar flare. The contribution from primary electrons is taken from Ref. [5]. One sees that trapped protons and electrons and primary protons and  $\alpha$ -particles are the drivers and need to be taken into account as a source term. All these components but  $\alpha$  are included in the MARS14 simulations and results are presented below.

Regular variations in solar activity during a so-called 11-year cycle give rise to variations in integral particle fluxes of GCR within a factor of 2 while the variations in their spectra in the energy range of 10 to 1000 MeV can be more significant. At solar flares the number of protons emitted from Sun can increase significantly thus disturbing Earth's magnetosphere. It gives rise to variations in orbit-averaged fluxes for both trapped particles and GCR. The GCR spectra for the largest solar flare ever observed (October 20, 1989) [3] are shown in Fig. 2. For more realistic estimate of absorbed dose, a model of ordinary solar flares of a lower magnitude should be taken into account.

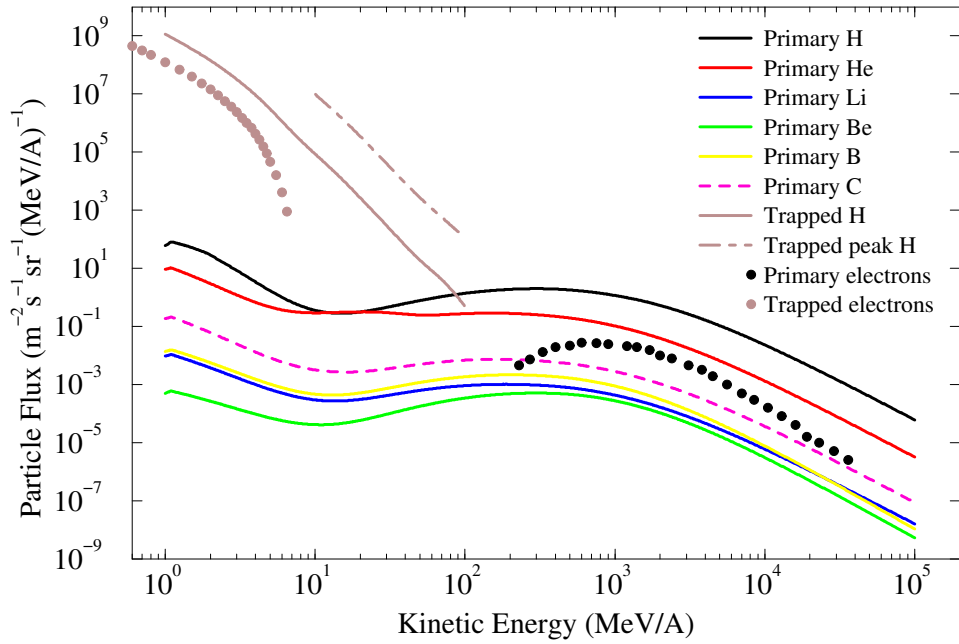


Figure 1: Orbit-averaged particle spectra, except “trapped peak”, at solar minimum. The highest level of trapped protons (“trapped peak”) is observed on a segment of the orbit near its perigee.

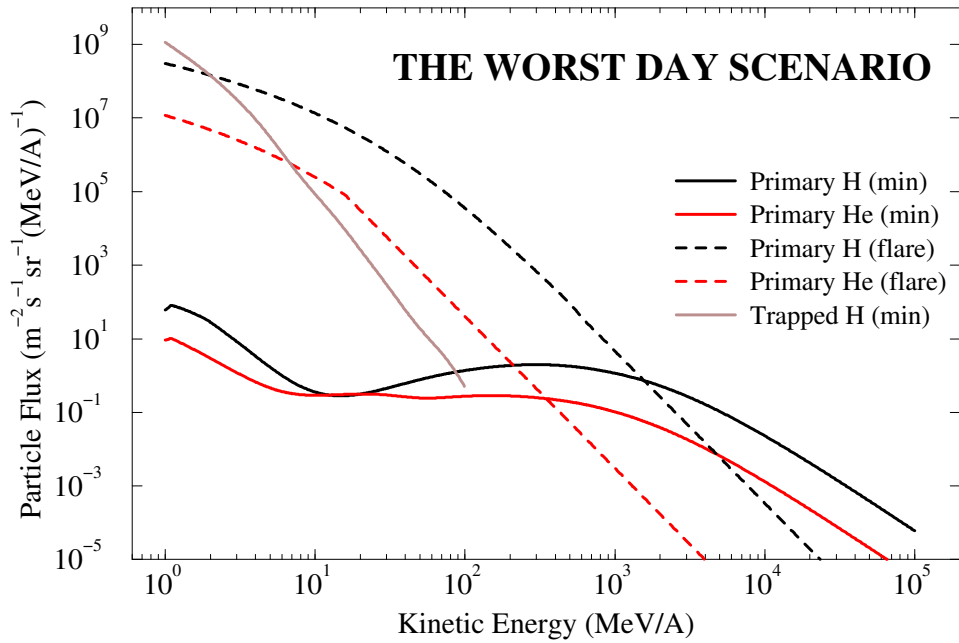


Figure 2: Orbit-averaged particle spectra at the largest solar flare ever detected.

### 3 Geometry and MARS Modeling

Calculations of radiation exposure of a SNAP CCD were performed for the orbit described above. Hadronic and electromagnetic showers induced in the apparatus by the sources described in the previous section are simulated with the MARS14 code in the energy range from 100 GeV down to 0.1 MeV.

In order to simplify the radiation model, a judgment was made regarding which parts of the SNAP satellite would be the most significant in terms of intercepting incoming cosmic radiation. Information about the SNAP conceptual design was obtained from the file S-14\_full\_assy.SLDASM in full\_assy\_model\_e\_test, downloaded from the LBNL engineering website [6]. The material through which a particle from the sun-side would pass would most likely consist of, at a minimum (“minimum” since lots of other smaller items on the spacecraft and attached to the optical bench may also be encountered):

- Multi-layer insulation (MLI) consisting of 30 layers of about 6 micron thick mylar, at a density of about 15 layers per cm, each layer coated on both sides with about 500 Å of aluminum. The MLI also includes a very low-density spacer (polyimide) between layers of mylar which is probably negligible.
- The optical bench, consisting of layers of 2 mm thick carbon-fiber “tooling plates”.
- The conical shield, material and thickness to be optimized within mass, space, structural and thermal constraints.

A few things are added to the above items in front, depending on the angle of approach:

- The spacecraft deck (if the angle is from below) consisting of carbon-fiber composite, probably 2-mm thick sheets like the optical bench.
- If the angle is from above, one has the following sequence: MLI, baffles (which are 1-mm thick aluminum), main mirror, optical bench box, and shield.

From the side opposite the Sun the situation is quite different; the thermal radiator is the main piece of material and appears to be essentially the only material. The present thermal radiator concept is 1.25-cm thick aluminum.

For this model, we begin with just the spacecraft deck, optical bench box, conical shield, and the cold plate supporting the CCD array. The simplified geometry model used in simulations is shown in Figs. 3 and 4. The satellite axis is along z-axis. The deck, optical bench box, and conical shield are assumed to be made of aluminum with thickness equal to 5.0, 2.5 and 2.0 cm, respectively. The cold plate is modeled as a molybdenum hexagon 2.5 cm in thickness. The opening in the optical bench box is modeled as a circular (R=30 cm) hole in the box (in xz-plane) with a center at  $y = -63$  cm and  $z = 75$  cm (Fig. 3).

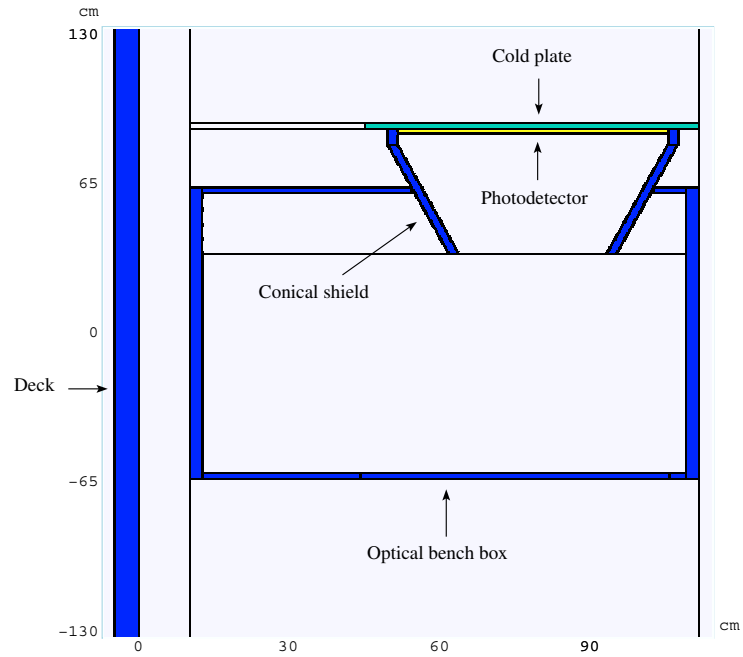


Figure 3: A fragment of the satellite MARS model (yz-view).

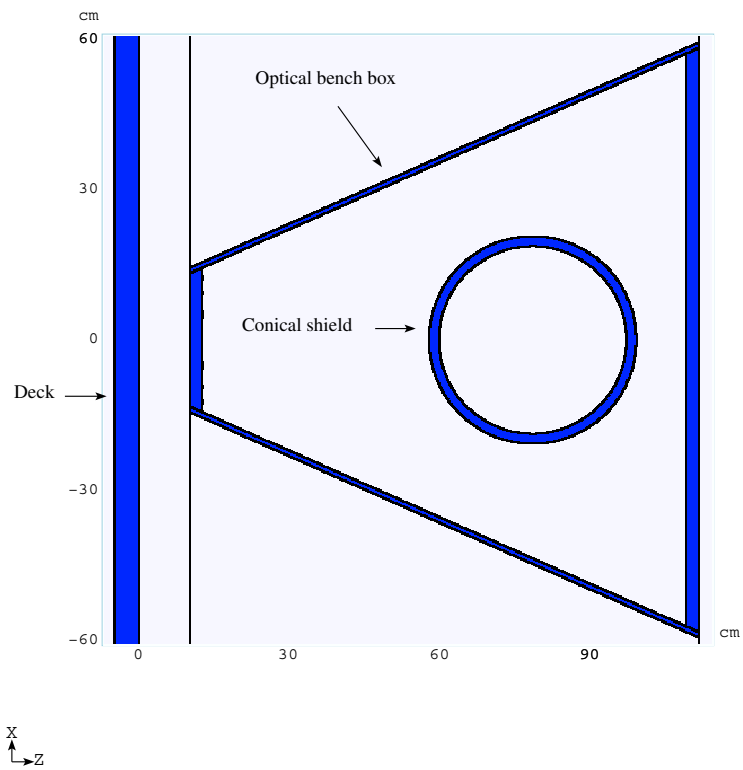


Figure 4: A fragment of the satellite MARS model (xz-view).

## 4 Dose Accumulated in CCD

In Monte Carlo calculations performed with the MARS14 code, the satellite is not considered to be orientation-stabilized and all the source terms are assumed to be isotropic. Three cases are considered:

1. Solar activity at minimum.
2. Solar activity at maximum.
3. The worst day scenario: the largest solar flare ever observed.

The particle spectra averaged over the CCD volume are presented in Figs. 5 and 6. One sees that there are many secondaries generated in the setup components, especially neutrons and photons, that can contribute to the radiation load in the CCD. The galactic protons dominate significantly over trapped ones in the photodetector.

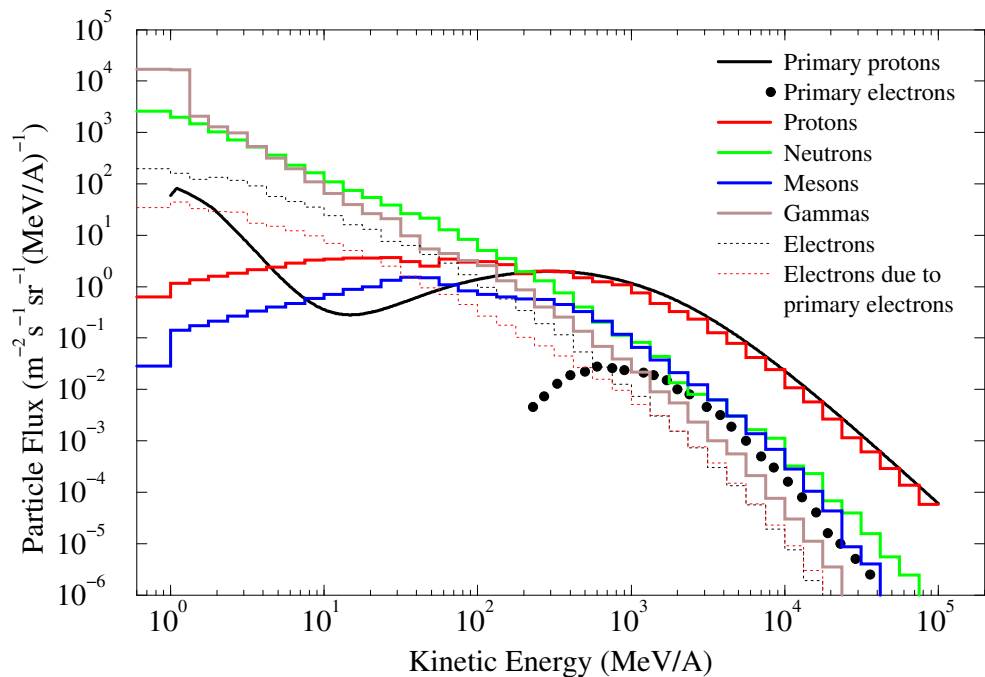


Figure 5: Particle spectra in CCD at solar minimum.

At the same time, the dose absorbed in the CCD during the worst day due to the largest solar flare equals to 4 rad, *i.e.* about 50% of the yearly dose due to primary protons at solar minimum (see Table 1). The dose values presented in Table 1 depend differently on the thickness of the model photodetector. When varying the thickness in a cm- and mm-region, negligible changes in the absorbed doses are observed for the “closed box” option.

For the box with an opening, however, the contribution from trapped radiation, both protons and electrons, varies almost inversely proportional with the thickness. It can be easily understood taking into account short ranges of low-energy protons and electrons that dominate in the trapped spectrum and are absorbed completely in the photodetector for the model with an opening.

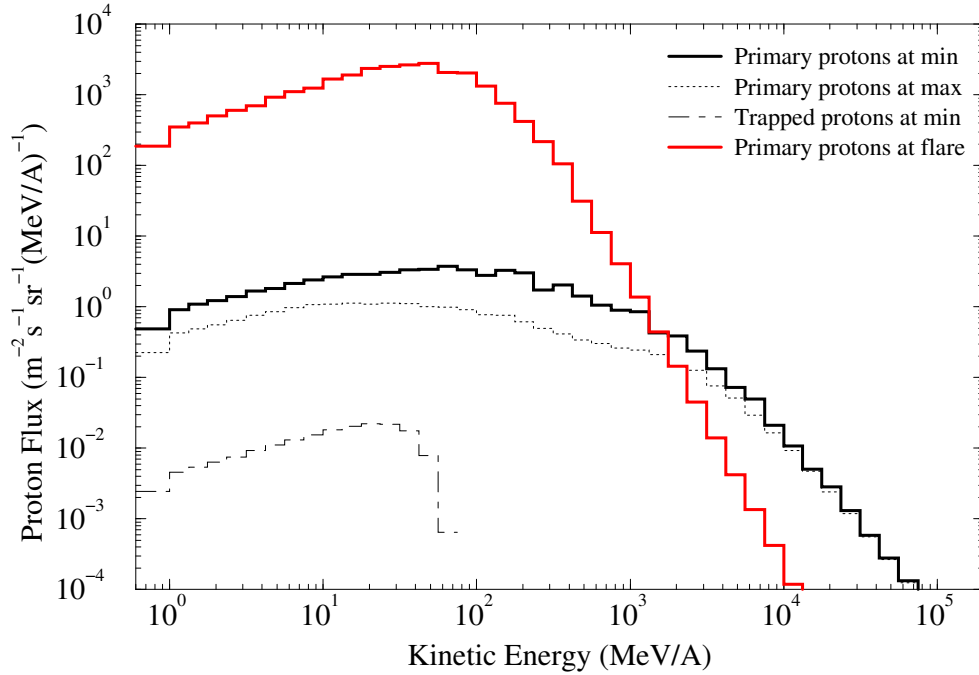


Figure 6: Proton spectra in CCD for different sources.

Table 1: Yearly absorbed dose (rad) in CCD.

Radiation source	Closed box	Box with an opening
Primary protons	7.7	8.3
Trapped protons	0.02	1390
Primary electrons	0.4	0.4
Trapped electrons	1.8	670
Total	10	2070

## 5 Verification

The CREME96 code [3] includes, in particular, routines for estimation of radiation attenuation by a shielding layer and absorbed dose in a silicon target. One of the routines, TRANS, keeps track of nuclear fragments produced by cosmic-ray projectiles. The routine, however, does not track low-energy and short-range fragments produced from target nuclei in shielding material itself. The results can be used for comparison with the detailed MARS calculations above.

Using the CREME96 built-in routines, we estimated absorbed dose in a silicon target shielded with a 3-cm aluminum layer. The yearly dose in such a target due to primary protons equals to 4.7 rad according to CREME96 and should be compared to the value of 7.7 rad in Table 1. Taking into account all the differences between the two models (simplified shielding in CREME96, different sensitive elements and different physical models

employed for particle interactions and transport in the two codes) the agreement is quite reasonable.

An estimate of the absorbed dose in a silicon shielded with a 3-cm aluminum layer was performed by means of CREME96 for a combined effect of primary protons and  $\alpha$ -particles. The yearly dose is up by 40% becoming 6.5 rad. Thus, taking  $\alpha$ -particles into account is mandatory for orbits and models where/when the contribution from primary cosmic rays dominates over that from the trapped protons.

## 6 Estimate of charge transfer efficiency degradation

Degradation of charge transfer efficiency (CTE) due to radiation damage is a major concern for such highly sensitive photodetectors as CCD. Table 2 gives predicted CTE degradation based on approximate separation of energy deposited in the detector into the ionizing and non-ionizing energy loss (NIEL). It is NIEL that gives rise to atomic displacements and generation of effective charge traps responsible for CTE degradation. For the estimate, we used the fact that 1 rad is approximately equivalent to  $10^{-3}$  non-ionizing rad (nirad) for proton radiation in such an environment [7]. Taking that into account and using the data from Table 1, one obtains the following yearly absorbed doses in CCD (only major radiation contributions are considered): (i) closed box option  $7.7 \times 0.754 = 5.80$  nirad (the factor of 0.754 equals to a neutron fraction in the total hadron flux over the volume of the CCD); (ii) box with an opening  $8.3 \times 0.754 + 1.39 = 7.65$  nirad. Further, we used the degradation rates specific to the two best devices developed at LBNL: standard high-resistivity devices and notch high-resistivity devices with  $\Delta\text{CTE}$  equal to  $2.5 \cdot 10^{-13}$  and  $9.6 \cdot 10^{-14}$  g/MeV, respectively [8]. Other devices have significantly higher degradation rates [8] and are not considered in the paper.

Table 2: Predicted degradation (%) of performance of a CCD photodetector with  $1024 \times 1024$  pixels for a 4-year mission. The upper and lower numbers refer to the optimistic ( $\Delta\text{CTE} = 9.6 \cdot 10^{-14}$  g/MeV) and pessimistic estimate ( $\Delta\text{CTE} = 2.5 \cdot 10^{-13}$  g/MeV), respectively. The degradation was calculated as  $1 - \text{CTE}^{1024}$ .

Radiation source	Closed box	Box with an opening
Protons	13	17
	31	39
Protons and $\alpha$ -particles	19	22
	42	48

One can see that the predicted CTE degradation for the LBNL notch high-resistivity devices is quite acceptable while other ones can hardly survive for the 4-year mission.

## 7 Conclusions

The analysis performed enabled us to get the first estimate of radiation load to the SNAP CCD in a simplified geometry model and for realistic radiation environment on the orbit. The following items should be refined in further studies:

1. Allowable limits for the CCD and electronics – radiation dose, total fluxes and background rates – to design shielding appropriately.
2. CCD specific: charge transfer efficiency *vs* accumulated dose.
3. Add more realism to the CCD detector model.
4. Add other components of the satellite.
5. Add and analyze on-board electronics that needs protection against radiation.
6. Clarify details (position, dimensions etc) of the opening in the optical bench box for incoming optical radiation.
7. Add accurate treatment of transport and interactions of  $\alpha$ -particles and possibly heavier ions.
8. Date of the beginning and duration of the mission; it is required to take into account a model of regular solar flares.

## 8 Acknowledgments

We are thankful to Fritz DeJongh for detailed info on orbit parameters and Peter Limon for useful comments.

## References

- [1] <http://snap.lbl.gov/>
- [2] N.V. Mokhov, “The MARS Code System User’s Guide”, Fermilab-FN-628 (1995); N.V. Mokhov, O.E. Krivosheev, “MARS Code Status”, Proc. Monte Carlo 2000 Conf., p. 943, Lisbon, October 23-26, 2000, Fermilab-Conf-00/181 (2000); N.V. Mokhov, “Status of MARS Code”, Fermilab-Conf-03/053 (2003); <http://www-ap.fnal.gov/MARS/>.
- [3] <http://crsp3.nrl.navy.mil/creme96/>
- [4] <http://www.spennis.oma.be/spennis/>
- [5] M. Aguilar *et al.* *Phys. Rep.* **366** (2002) 331-405.
- [6] <http://www-eng.lbl.gov/hoff/>

- [7] J.E. Nealy, G.D. Qualls, L.C. Simonsen, "Integrated shield design methodology: application to a satellite instrument", in Proc. NASA Workshop on shielding strategies for human space exploration, Houston, Texas, December 6-8, 1995; NASA Conference Publication 3360, December 1997, p.385-396.
- [8] C. Bebek, D. Groom, S. Holland *et al.*, "Proton radiation damage in P-channel CCDs fabricated on high-resistivity silicon", [http://snap.lbl.gov/pubdocs/CCDpaper\\_rev2.pdf](http://snap.lbl.gov/pubdocs/CCDpaper_rev2.pdf)